

Step-by-Step Video-to-Audio Synthesis via Negative Audio Guidance

Akio Hayakawa¹ Masato Ishii¹ Takashi Shibuya¹ Yuki Mitsufuji^{1,2}

¹Sony AI ²Sony Group Corporation

{akio.hayakawa, masato.a.ishii, takashi.tak.shibuya, yuhki.mitsufuji}@sony.com

Abstract

We propose a novel step-by-step video-to-audio generation method that sequentially produces individual audio tracks, each corresponding to a specific sound event in the video. Our approach mirrors traditional Foley workflows, aiming to capture all sound events induced by a given video comprehensively. Each generation step is formulated as a guided video-to-audio synthesis task, conditioned on a target text prompt and previously generated audio tracks. This design is inspired by the idea of concept negation from prior compositional generation frameworks. To enable this guided generation, we introduce a training framework that leverages pre-trained video-to-audio models and eliminates the need for specialized paired datasets, allowing training on more accessible data. Experimental results demonstrate that our method generates multiple semantically distinct audio tracks for a single input video, leading to higher-quality composite audio synthesis than existing baselines.

1 Introduction

We are interested in generating audio signals that align seamlessly with a given video—a process commonly referred to as Foley in film production [Ament, 2021]. Foley artists meticulously create sound effects by selecting or recording sounds for each audible event in a video, followed by careful mixing to ensure proper temporal and contextual alignment. While essential for producing high-quality audiovisual content, this process is highly labor-intensive and time-consuming, as even short video clips often contain numerous audible events.

Advancements in video-to-audio generation models [Viertola et al., 2025, Luo et al., 2023, Wang et al., 2024b,a, Liu et al., 2024, Cheng et al., 2025, Polyak et al., 2024] have shown promise in automating this workflow. These models can generate high-quality audio that aligns semantically and temporally with the given video. However, unlike the traditional Foley workflow, they typically generate an entire audio track at once without an explicit mixing process. This lack of modularity poses a significant challenge. When the generated audio is unsatisfactory, creators have no choice but to regenerate the entire track, even if only specific elements are incorrect or missing. Such inefficiencies limit the practical application of these models, particularly in collaborative workflows with human creators.

We argue that a step-by-step generation mechanism is crucial to making video-to-audio synthesis more practical and adaptable. Instead of generating the entire audio track at once, a model should iteratively produce individual audio tracks, focusing on one sound event at a time, as illustrated in Fig. 1. This strategy closely mirrors the traditional Foley workflow, offering greater control and efficiency in the sound creation process.

In this paper, we propose a novel guided generation method, Negative Audio Guidance (NAG), for the step-by-step video-to-audio synthesis. NAG enables the generation of specific audio events that are missing from the current audio tracks, guided by a text prompt. By iteratively applying this

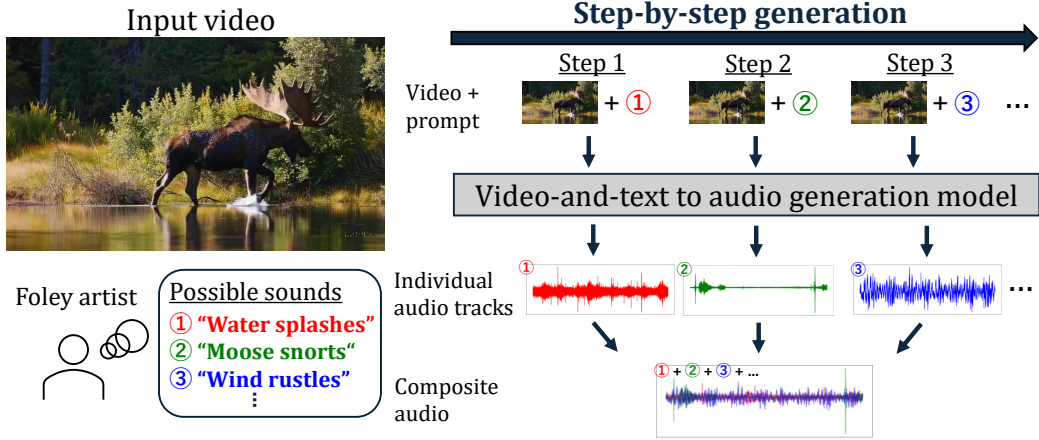


Figure 1: Step-by-step video-to-audio generation for compositional sound effect creation. Video often contains numerous audible events, and Foley artists synthesize composite audio by adding missing audio components step-by-step. Supporting this step-by-step generation with a video-to-audio generation model offers greater control and efficiency in sound creation.

guided generation process, a model progressively builds a composite audio that covers all relevant sound events in the video. We also design a training framework for the additional guidance term based on pre-trained video-to-audio models. This eliminates the need for specialized training datasets, specifically, the difficult-to-obtain pairs of multiple plausible audio tracks for a single video. Extensive experiments demonstrate that our method successfully generates individual audio tracks step-by-step while maintaining the quality of the final audio output.

2 Related work

2.1 Video-to-audio synthesis

The goal of video-to-audio synthesis is to generate an audio signal that aligns semantically and temporally with an input video. Early approaches used regression models [Chen et al., 2020b] and GANs [Iashin and Rahtu, 2021], while more recent ones have adopted autoregressive models [Viertola et al., 2025] and diffusion models [Luo et al., 2023, Wang et al., 2024b,a, Liu et al., 2024, Cheng et al., 2025, Polyak et al., 2024] due to their high capability in generation tasks. However, these models typically accept only videos (and optionally text prompts) as input conditions, making it impossible to specify sounds that users may want to combine with the generated audio.

Few studies have explored audio conditioning in video-to-audio synthesis to address their respective problem setting. MultiFoley [Chen et al., 2024b] uses conditional audio as reference audio to be included in the generated audio. Sketch2Sound [García et al., 2025] takes a similar approach, but only uses a particular set of signal features extracted from the original conditional audio to accept sonic or vocal imitations as conditions. Action2Sound [Chen et al., 2024a] puts more focus on the disentanglement of foreground and ambient sound, and the conditional audio is used to specify the ambient sound to appear in the generated audio. Different from these studies, we use audio conditioning to specify what kind of audio *should not* appear in the generated audio, enabling step-by-step generation in video-to-audio synthesis.

2.2 Generative "add" operation

Generative "add" operations in the audio domain are executed to generate audio that can be mixed with an input audio signal, often guided by a text prompt. These operations have been explored in text-to-audio [Wang et al., 2023, Jia et al., 2025] and text-to-music [Han et al., 2024, Parker et al., 2024, Mariani et al., 2024, Postolache et al., 2024, Karchkhadze et al., 2025] synthesis and can be divided into two approaches: training-based and training-free.

In the training-based approach, the model is explicitly trained to perform the "add" operation given the input audio. This training requires a triplet comprising an input audio, a text prompt, and an audio to be added as training data [Wang et al., 2023, Han et al., 2024, Parker et al., 2024]. Unfortunately, existing methods are difficult to apply in our setting because such data is hard to obtain. Even within a single scene, a mixture of many sounds can be observed, and separating them into individual ones is challenging [Owens and Efros, 2018, Zhu and Rahtu, 2020, Song and Zhang, 2023].

On the other hand, the training-free approach is more flexible as it leverages a pre-trained text-to-audio/music model without any specific training process. The "add" operation is conducted as a partial generation of multi-track audio [Mariani et al., 2024, Postolache et al., 2024, Karchkhadze et al., 2025] or a re-generation with a target prompt from structured noise obtained through inverting the input audio [Jia et al., 2025]. Instead of specific training data, these methods require particular properties in the pre-trained model: multi-track joint generation [Mariani et al., 2024, Karchkhadze et al., 2025], data-space diffusion models [Postolache et al., 2024], and specific types of model architectures [Jia et al., 2025], which limit their applicability to our video-to-audio setting.

Similar "add" operations have been explored as object insertion in computer vision, where models generate an object image to be added to an input background image. They are also categorized into training-based [Singh et al., 2024, Canberk et al., 2024] and training-free approaches [Tewel et al., 2025], but in either case, they rely on segmentation models to create training data or guide the generation process. It means that a particular subset of pixels in the image is assumed to be wholly replaced with the generated one through the "add" operation. As "add" in the audio domain involves mixing rather than replacing, these approaches cannot be directly applied to our setting.

We took the training-based approach for this study to conduct the "add" operation in the audio domain and designed our framework to eliminate the necessity of special types of training data. This makes this approach more practical and adaptable to video-to-audio synthesis tasks.

3 Method

3.1 Preliminaries

Generative modeling with flow-matching

Let $p_1(x)$ be a data distribution where $x \in \mathbb{R}^d$. Flow matching [Lipman et al., 2023] considers the probability flow ODE $\frac{d}{dt}\phi_t(x) = u_t(\phi_t(x))$, where $t \in [0, 1]$ is a timestep, u_t is the velocity field, and $\phi_t(x) = \phi(x, t) : \mathbb{R}^d \times \mathbb{R} \rightarrow \mathbb{R}^d$ is the flow that maps x to the intermediate data x_t . ϕ_t can be an arbitrary function that satisfies the terminal condition $\phi_1(x_1) = x_1$ and $\phi_0(x_1) \sim p_0$, where p_0 is a tractable distribution such as a standard normal distribution $\mathcal{N}(0, I)$. Following the most popular setting, we define $\phi_t(x_1) = tx_1 + (1 - t)x_0$, where $x_0 \sim \mathcal{N}(0, I)$, resulting in $u(\phi_t(x)) = x_1 - x_0$.

Solving ODE from $t = 0$ to 1 with an initial sample $x_0 \sim p_0(x)$ enables sampling from the target data distribution $x_1 \sim p_1(x)$. To do this, a neural network is trained to predict $u_t(\phi_t(x))$, which corresponds to $x_1 - x_0$ in our case, through minimizing the squared error over data and timesteps. In text-conditioned video-to-audio synthesis, the model takes additional conditional inputs, which are input video V and text prompt C , to model a conditional flow $u_t(\phi_t(x)|V, C)$.

Guidance for flow-matching models with multiple conditions

Classifier-free guidance [Ho and Salimans, 2021] is widely used to improve generation quality and fidelity to conditions. This guidance is usually conducted with a single condition, and it is not trivial how to conduct it with two conditions, as in text-conditioned video-to-audio synthesis. To derive a proper guidance process, $p(x|V, C)$ is decomposed as the following equation:

$$p(x|V, C) = p(x) \left(\frac{p(x|V)}{p(x)} \right) \left(\frac{p(x|V, C)}{p(x|V)} \right). \quad (1)$$

On the basis of this decomposition, Kushwaha and Tian [2025] proposed the following guided flow:

$$\begin{aligned} \tilde{u}_\theta(x_t) = & u_\theta(x_t, t, \emptyset, \emptyset) + w_1(u_\theta(x_t, t, V, \emptyset) - u_\theta(x_t, t, \emptyset, \emptyset)) \\ & + w_2(u_\theta(x_t, t, V, C) - u_\theta(x_t, t, V, \emptyset)), \end{aligned} \quad (2)$$

where θ is a set of the model parameters, and \emptyset denotes a null condition. The three terms of the right-hand side of Eq. (2) respectively correspond to the three factors on the right-hand side of Eq. (1). They empirically show that setting $w_1 = w_2$ achieves better results, and in this case, $u_\theta(x_t, t, V, \emptyset)$ cancels out, which gives us the following simplified formulation:

$$\tilde{u}_\theta(x_t) = u_\theta(x_t, t, \emptyset, \emptyset) + w_1(u_\theta(x_t, t, V, C) - u_\theta(x_t, t, \emptyset, \emptyset)). \quad (3)$$

3.2 Problem setup: step-by-step generation in video-to-audio synthesis

We are interested in iteratively generating individual audio tracks, focusing on one sound event at a time. We assume two tracks for simplicity in the theoretical formulation, denoted as $x^{(1)}$ and $x^{(2)}$. We also assume that text prompts C_1 and C_2 are provided to specify the sound event associated with each track. As C_1 and C_2 describe two distinct sound events, $x^{(2)}$ should not contain any sound concepts related to $x^{(1)}$, and vice versa.

In this setting, our goal is to sample $x^{(1)}$ and $x^{(2)}$ from $p(x^{(1)}, x^{(2)} | V, C_1, C_2)$ in a step-by-step manner. To achieve this, we approximate the target distribution as follows:

$$(x^{(1)}, x^{(2)}) \sim p(x^{(1)}, x^{(2)} | V, C_1, C_2) \quad (4)$$

$$\begin{aligned} &= p(x^{(1)} | V, C_1, C_2) p(x^{(2)} | V, C_1, C_2, x^{(1)}) \\ &\approx p(x^{(1)} | V, C_1) p(x^{(2)} | V, C_2, x^{(1)}). \end{aligned} \quad (5)$$

This approximation gives us an intuition on sequential sampling of $x^{(1)}$ and $x^{(2)}$ from the target distribution.

Sampling $x^{(1)}$: Theoretically speaking, we need to sample it from $p(x^{(1)} | V, C_1, C_2)$. However, obtaining C_2 before sampling $x^{(1)}$ may not be feasible because, in practice, C_2 could be specified by a user after $x^{(1)}$ is generated. Therefore, we dropped C_2 through the approximation, which leads to $p(x^{(1)} | V, C_1)$. Sampling from this distribution is common with a standard text-conditional video-to-audio synthesis; thus, we can conduct it with existing video-to-audio models.

Sampling $x^{(2)}$: As we can expect that $x^{(1)}$ contains all the information of C_1 , meaning that it is a sufficient statistic, the distribution of $x^{(2)}$ becomes $p(x^{(2)} | V, C_2, x^{(1)})$. From a straightforward standpoint, learning to generate samples from this distribution would require tuples of $(x^{(2)}, V, C_2, x^{(1)})$ as training data. Unfortunately, constructing such data from a video is a challenging task called visually-guided audio source separation [Owens and Efros, 2018, Zhu and Rahtu, 2020, Song and Zhang, 2023], and thus we cannot expect high-quality training datasets. Instead, we propose a new training framework to eliminate the necessity of such specialized data.

Note that this setup can be applied even when there are three or more sound events. When generating the k -th audio track, we can set the mix of the previously generated $(k - 1)$ audio tracks as $x^{(1)}$, and use it to sample $x^{(2)}$. Please refer to Section 5.1 for more details of this procedure.

3.3 Formulation of target distribution with concept negation

Recall that we want to generate $x^{(2)}$ to cover a missing sound event in $x^{(1)}$. In this sense, conditioning by $x^{(1)}$ corresponds to a concept negation [Du et al., 2020, Liu et al., 2022, Valle et al., 2025] in generating $x^{(2)}$; the generated $x^{(2)}$ *should not* contain any concepts related to $x^{(1)}$. We denote this type of audio condition as $\bar{\mathcal{E}}(\cdot) = \neg \mathcal{E}(\cdot)$ to explicitly differentiate it from a standard type of audio condition denoted by $\mathcal{E}(\cdot)$. Based on the above-mentioned relationship between $x^{(1)}$ and $x^{(2)}$, we approximate the target distribution of $x^{(2)}$ using the concept negation as follows:

$$p(x^{(2)} | V, C_2, x^{(1)}) \approx p(x^{(2)} | V, C_2, \bar{\mathcal{E}}(x^{(1)})). \quad (6)$$

Following the study by Du et al. [2020], we assume that the concept negation holds this property:

$$p(x, c_p, \neg c_n) \propto p(x) p(c_p | x) p(c_n | x)^{-1}, \quad (7)$$

where c_p and c_n denote conditional concepts to generate x .

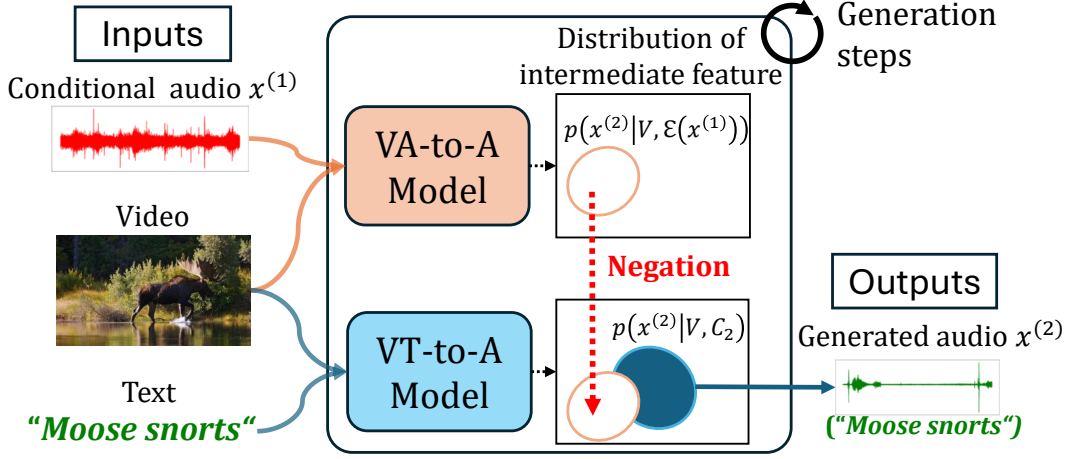


Figure 2: Overview of the proposed method. Each audio track should represent a distinct audio event. Using previously generated audio tracks as a condition for the negation concept, we explicitly push the current generation process away from the audio tracks already generated.

To derive our guidance, we decompose the target distribution using Eq. (7) and Bayes’ theorem as:

$$\begin{aligned}
 p(x^{(2)} | V, C_2, \bar{\mathcal{E}}(x^{(1)})) &\propto p(x^{(2)}, V, C_2, \bar{\mathcal{E}}(x^{(1)})) \\
 &\propto p(x^{(2)}, V) p(C_2 | x^{(2)}, V) p(\mathcal{E}(x^{(1)}) | x^{(2)}, V)^{-1} \\
 &\propto p(x^{(2)}) \left(\frac{p(x^{(2)} | V)}{p(x^{(2)})} \right) \left(\frac{p(x^{(2)} | V, C_2)}{p(x^{(2)} | V)} \right) \left(\frac{p(x^{(2)} | V)}{p(x^{(2)} | V, \mathcal{E}(x^{(1)}))} \right). \quad (8)
 \end{aligned}$$

Similar to the derivation of Eq. (2), we can derive the guidance process based on this decomposition, as shown in the next section. It indicates we can sample $x^{(2)}$ using this new guidance with flow matching models. Iterating this process enables step-by-step generation in video-to-audio synthesis.

4 Implementation

4.1 Guided flow for step-by-step generation

The decomposition shown in Eq. (8) yields a new guidance formulation comprising four terms: one unconditional flow term and three guidance terms. However, adjusting the coefficients of the three guidance terms is cumbersome in practice. Given the empirical results [Kushwaha and Tian, 2025], where simplifying the guidance by removing $u_\theta(x_t, t, V, \emptyset)$ in Eq. (2) performs well, we also set the guidance coefficients so that $u_\theta(x_t, t, V, \emptyset)$ cancels out for simplification. Specifically, we set the sum of the coefficients of the first and third guidance terms to equal the coefficient of the second guidance term (see supplemental materials for more details). This leads to the following guided flow:

$$\begin{aligned}
 \tilde{u}_{\theta, \psi}(x_t) &= u_\theta(x_t, t, \emptyset, \emptyset) + \alpha(u_\theta(x_t, t, V, C_2) - u_\theta(x_t, t, \emptyset, \emptyset)) \\
 &\quad + \beta(u_\theta(x_t, t, V, C_2) - u_{\theta, \psi}(x_t, t, V, \emptyset, x^{(1)})), \quad (9)
 \end{aligned}$$

where α and β are the coefficients of the guidance terms. As we need an audio-conditioned flow in the last term, we introduce an additional set of trainable parameters ψ to adapt the text-conditioned video-to-audio model to predict it, as we show its details in the next subsection.

The second term on the right-hand side of Eq. (9) corresponds to a standard guidance term in text-conditioned video-to-audio models, which appeared in Eq. (3). It strengthens the fidelity of the generated audio to the conditional video and text prompt. The third term is a new guidance term appearing in our proposed method, which pushes the generated audio away from the conditional audio $x^{(1)}$. This prevents the already generated audio events from being re-generated in the current

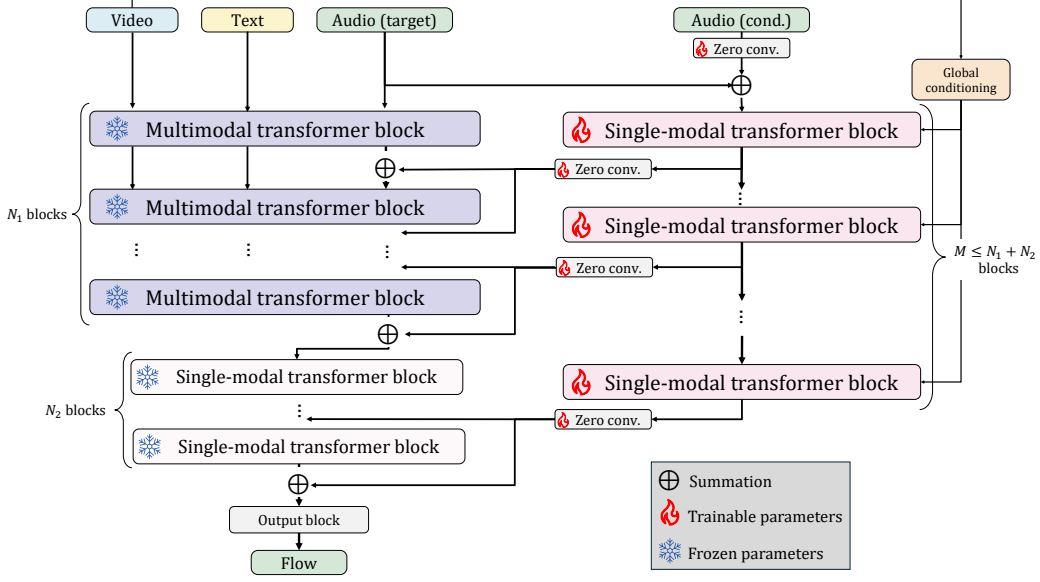


Figure 3: Overview of network architecture for the audio-conditional flow estimator. We adopt ControlNet for the multi-modal diffusion transformer (MM-DiT) to incorporate audio condition into the pre-trained MMAudio.

generation step, enabling step-by-step generation without overlapping audio events. Since $x^{(1)}$ is used similarly for a negative prompt, we refer to this new guidance as Negative Audio Guidance (NAG).

4.2 Training flow estimator for Negative Audio Guidance

All the flows appearing on the right-hand side of Eq. (9), except for the last one, can be estimated using standard text-conditional video-to-audio models. The remaining term is a conditional flow corresponding to the distribution $p(x^{(2)}|V, \mathcal{E}(x^{(1)}))$. As $\mathcal{E}(\cdot)$ is a standard type of audio conditioning, this flow estimator can be seen as an extended version of the video-to-audio model, enhanced by incorporating conditional audio as an additional input. Therefore, we train the flow estimator using ControlNet [Zhang et al., 2023] parameterized by ψ . As a base video-to-audio model, we used MMAudio, parameterized by θ , for its high capability in video-to-audio synthesis.

Model architecture Figure 3 shows an overview of the ControlNet architecture of the flow estimator. Since MMAudio uses a sophisticated architecture extended from MM-DiT [Esser et al., 2024], we adapt the architecture of ControlNet accordingly. Inspired by Stable Diffusion 3.5 [Stability-AI, 2024], we stack several single-modal transformer blocks to extract features from the conditional audio, and the features extracted at each block are added to the intermediate features of the corresponding blocks in MMAudio. During training, we freeze the pre-trained parameters of MMAudio and only update the parameters of the additional modules.

Training dataset We follow the training strategy of MMAudio; we jointly used both text-video-audio and text-audio paired datasets for training. Specifically, we used VGGSound [Chen et al., 2020a] as a text-video-audio dataset, while Clotho [Drossos et al., 2020], AudioCaps [Kim et al., 2019], and WavCaps [Mei et al., 2024] were used as text-audio datasets. From each audio clip, we sampled a four-second audio segment as x^{tgt} and another one as x^{cond} so that the two segments do not overlap. We also extracted a video segment corresponding to x^{tgt} as a conditional video V when the data came from VGGSound; otherwise, we set the pretrained empty token of MMAudio as V . Then, the sampled clips were used to compute the flow $u_{\theta, \psi}(x_t^{\text{tgt}}, t, V, \emptyset, x^{\text{cond}})$, and ψ is optimized by minimizing the flow-matching loss.

5 Experiments

5.1 Evaluation setup

Multi-Caps VGGSound: multi-captioned audio-video dataset for evaluation We constructed a new audiovisual dataset called Multi-Caps VGGSound to evaluate the step-by-step video-to-audio generation. We generated five captions using Qwen2.5-VL [Bai et al., 2025] for each video in the test split of the VGGSound dataset, comprising 15,221 video clips in total. We instructed the model to generate captions, each describing a different sound event that could appear in the input video’s audio tracks, including both foreground and background audio. Since Qwen2.5-VL does not accept audio as input, these captions were created solely based on the visual input without considering the original audio of the input video. We provide more details in the supplemental materials.

Task setup: Step-by-step audio generation We generated five audio tracks $\{x^{(k)}|k \in \{1, 2, \dots, 5\}\}$ corresponding to audio captions $\{C_k|k \in \{1, 2, \dots, 5\}\}$ for each video V in the Multi-Caps VGGSound dataset. We took the first eight-second segment from the video and generated sounds for this segment using different captions. Given the multiple generated audio tracks, we synthesized a composite audio \tilde{x} by $\tilde{x} = \text{normalize}(\sum_k x^{(k)})$. We used the loudness normalization [Steinmetz and Reiss, 2021] for the composition so that the total loudness would not deviate from that of natural audio. The target loudness was set to -20 LUFS, which corresponds to the mean loudness of the VGGSound test dataset.

Step-by-step audio generation with NAG To generate the audio tracks step-by-step using NAG, we used the composite audio of all audio tracks generated in the previous generation steps as a condition for NAG. Specifically, at the generation step for $x^{(k)}$, we synthesized a composite audio $\tilde{x}_{:k} = \text{normalize}(\sum_{l=1}^{k-1} x^{(l)})$ for the condition. Since no audio track was already generated when generating the first audio, we generated it using the standard classifier-free guidance in Eq. (3). We empirically set $\alpha = 4.5$ and $\beta = 1.5$ in Eq. (9) (see the supplemental materials for more details).

Baseline models We compared our proposed method with several open-sourced text-and-video conditional audio (TV2A) generation models. We chose each State-of-the-Art TV2A model among various training approaches: Seeing-and-Hearing [Xing et al., 2024] as a TV2A model adapted from the T2A model in a zero-shot manner, FoleyCrafter [Zhang et al., 2024] as a TV2A model adapted from the T2A model through fine-tuning, and MMAudio [Cheng et al., 2025] as a TV2A model trained from scratch. Note that our model is built upon MMAudio with additional audio conditions introduced by the proposed ControlNet architecture. We compared the proposed NAG to the original MMAudio-S-16k model with the classifier-free guidance (CFG) or negative prompting.

We tested two generation processes to generate multiple audio tracks and obtain a composite audio using the baseline models: independent generation and step-by-step generation based on negative prompts. In the independent generation, we generated five sounds for each video using different text conditions. In this case, each generation process does not access the other audio tracks or their corresponding captions. In the step-by-step generation based on negative prompts, we generated each audio track with negative prompting [Woelf, 2022] to make it far away from all the captions used at the previous generation steps. Specifically, for the video V with the k -th audio caption C_k , we computed the guided flow by $\tilde{u}_\theta(x_t) = u_\theta(x_t, t, \emptyset, \emptyset) + w_1(u_\theta(x_t, t, V, C_k) - u_\theta(x_t, t, \emptyset, C_{k,\text{neg}}))$ at each timestep, where $C_{k,\text{neg}}$ is the concatenation of the other captions $\{C_l|l < k\}$.

Evaluation metrics We assessed the quality of both the composite audio and the individual audio tracks to evaluate the step-by-step audio generation.

Following the prior work [Cheng et al., 2025], we evaluated the composite audio in terms of audio quality, semantic alignment, and temporal alignment. We assessed the audio quality of the generated audio using Fréchet Distance (FD), Kullback–Leibler (KL) distance, and Inception Score (IS) [Salimans et al., 2016]. We used PANNs [Kong et al., 2020] (FD_{PANNs}) and VGGish [Gemmeke et al., 2017] (FD_{VGG}) for computing FD, and PANNs (KL_{PANNs}) and PaSST (KL_{PaSST}) for computing KL, and PANNs for computing IS, respectively. We assessed the semantic alignment between the input video and the composite audio by the cosine similarity between their embeddings extracted by ImageBind [Girdhar et al., 2023] (IB-score). We assessed the temporal alignment between the input

Method	Audio Quality					Semantic Align.	Temporal Align.
	FD _{PANNs} ↓	FD _{VGG} ↓	KL _{PANNs} ↓	KL _{PaSST} ↓	IS↑	IB-score↑	DeSync↓
One-Step Generation with Fused Caption (Reference as no individual audio track is available)							
Seeing-and-Hearing	25.42	5.68	2.81	2.76	6.45	36.88	1.22
FoleyCrafter	16.93	2.29	2.60	2.52	11.93	27.78	1.23
MMAudio-S-16k	6.75	1.03	2.09	2.04	13.66	29.45	0.46
Independent Generation							
Seeing-and-Hearing	31.81	7.68	3.10	2.65	4.12	20.16	1.19
FoleyCrafter	20.04	3.23	2.70	2.36	9.21	25.26	1.18
MMAudio-S-16k	7.76	1.35	2.02	1.84	10.42	28.13	0.42
Step-by-Step Generation with Negative Prompting							
FoleyCrafter	22.34	4.64	2.94	2.47	6.02	18.83	1.19
MMAudio-S-16k	9.53	1.89	2.21	1.94	8.72	25.06	0.45
Step-by-Step Generation with Negative Audio Guidance							
Ours	7.32	1.24	2.02	1.78	10.21	28.15	0.42

Table 1: Quantitative evaluation of the composite audio synthesized from the generated multiple audio tracks. The results of one-step generation using a fused caption are shown as a reference.

video and the generated audio with Synchformer [Iashin et al., 2024] (DeSync), where we took two 4.8-second segments at the beginning and end and averaged their scores.

For the evaluation on each audio track, we assessed its quality from four aspects: audio independency between the audio tracks generated for the same video, audio quality, audio-text alignment, and audio-video alignment of each audio track. Since distinct audio components should be represented in separate audio tracks, each generated audio track should differ from the other tracks. To evaluate audio independence, we computed the similarity between the CLAP [Wu et al., 2023] audio embeddings for each pair of audio tracks (10 pairs per video). For Audio-Text alignment, we computed the similarity between CLAP text embeddings from the input prompts (used to generate each audio track) and the corresponding CLAP audio embeddings. For audio quality and audio-video alignment, we adopted IS and IB-score, respectively, as in the composite audio evaluation protocol.

5.2 Main results

Evaluation on the composite audio Table 1 shows the quantitative evaluation of the composite audio. Our proposed method achieves the best results for all metrics except IS among all the methods. We also evaluated the generated samples by using the baseline models’ one-step generation with the caption created by fusing the five captions for each video. Though this generation process does not provide each audio track and differs from our goal of step-by-step generation, these values indicate the best possible scores of each baseline model.

Evaluation on each audio track Table 2 shows the quantitative evaluation of the individual audio tracks. The vanilla MMAudio-S-16k with CFG struggles to generate well-separated sounds for each audio track, which is shown as a worse audio independency score, although it achieves high audio quality and A-V Alignment. Using negative prompting improves the audio independency but drastically degrades all the other scores. Using NAG also successfully improves the audio independency while maintaining high audio quality and A-V alignment. The A-T alignment score marginally improves from that of the vanilla MMAudio, which we hypothesize that less contamination of other audio concepts results in a better A-T alignment score.

Figure 4 visually compares these three methods. The first audio track is the same in all methods, since it is generated by using only CFG. The vanilla MMAudio-S-16k tends to generate similar audio for multiple audio tracks. All generated audio tracks by the vanilla MMAudio-S-16k contain the sound of water as the moose walks (visually shown as vertical segments that appear at regular intervals). Since the moose and its movement are prominent in the input video, MMAudio tends to include the sound related to them regardless of the input text prompt. This is also reflected in the higher IB-score, indicating that all audio tracks are semantically aligned with the input video, regardless of whether the input prompt represents background audio (as in the case of the second audio track). Using

Method	Audio Independency	Audio Quality	A-T Align.	A-V Align.
	CLAP A-A↓	IS↑	CLAP T-A↑	IB-score↑
MMAudio-S-16k	79.75	12.47	28.36	27.76
MMAudio-S-16K + Neg. Prompting	75.37	11.71	27.14	25.85
MMAudio-S-16K + NAG (Ours)	74.74	12.00	28.79	26.44

Table 2: Quantitative evaluation of individual audio tracks. Our proposed method successfully improve audio independency among multiple tracks while maintaining other scores.

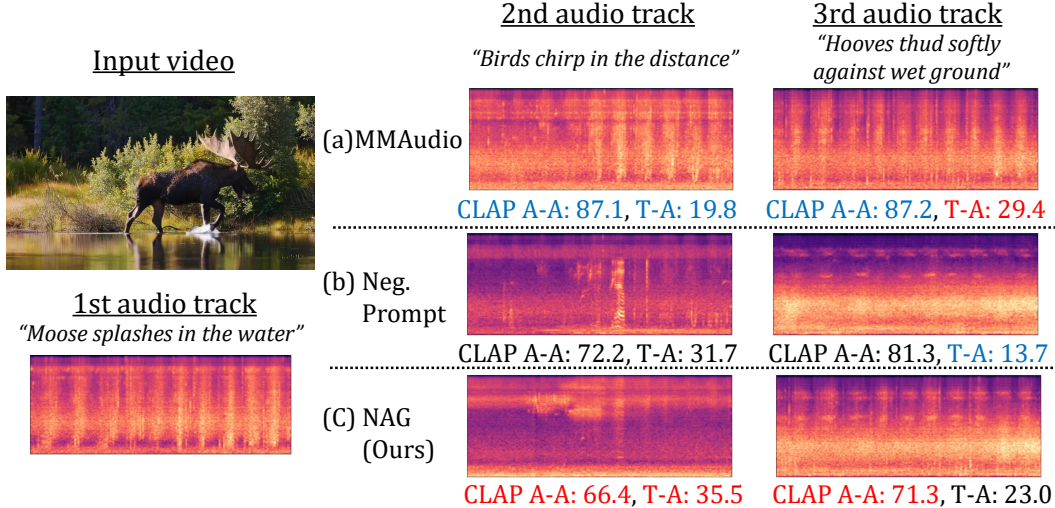


Figure 4: Spectrogram visualizations of step-by-step audio generation using (a) vanilla MMAudio, (b) MMAudio with negative prompting, and (c) MMAudio with Negative Audio Guidance (NAG). The first audio track is generated using (a) in all settings, resulting in identical outputs. Our proposed method effectively suppresses previously generated sounds in subsequent steps (second and third tracks) while maintaining high alignment with the target text prompts. The best and worst CLAP A-A and T-A scores are highlighted in red and blue, respectively.

negative prompting suppressed this contamination of the audio content, but it tends to suffer from worse text alignment. In contrast, the proposed NAG successfully suppressed the audio components already generated in the early generation steps while achieving better text alignment. It generates the missing sound specified by the text prompt by explicitly letting the generation process be away from the already generated sounds. We provide more generated samples in the supplemental materials.

6 Conclusion

We introduced a novel video-to-audio generation method, guided by text, video, and audio conditions, to enable step-by-step synthesis. By applying negative audio guidance alongside a text prompt, our approach generates multiple well-separated audio tracks for the same video input, facilitating high-quality composite audio synthesis. Importantly, our method does not require specialized training datasets. We built it on a pre-trained video-to-audio model by adapting ControlNet for audio conditioning, which can be trained on accessible datasets.

In this work, we synthesized composite audio using a simple mixing strategy, summing multiple audio tracks without weighting them, followed by loudness normalization. While effective, it does not account for the natural loudness of each audio track and might be suboptimal. As the optimal mixing can differ by video and audio content, incorporating a generative model to support this process could further enhance the quality of the composite audio. We leave this direction for future work.

References

- Vanessa Theme Ament. *The Foley Grail: The Art of Performing Sound for Film, Games, and Animation*. Routledge, 2021.
- Shuai Bai, Keqin Chen, Xuejing Liu, Jialin Wang, Wenbin Ge, Sibbo Song, Kai Dang, Peng Wang, Shijie Wang, Jun Tang, Humen Zhong, Yuanzhi Zhu, Mingkun Yang, Zhaohai Li, Jianqiang Wan, Pengfei Wang, Wei Ding, Zheren Fu, Yiheng Xu, Jiabo Ye, Xi Zhang, Tianbao Xie, Zesen Cheng, Hang Zhang, Zhibo Yang, Haiyang Xu, and Junyang Lin. Qwen2.5-vl technical report. *arXiv preprint arXiv:2502.13923*, 2025.
- Alper Canberk, Maksym Bondarenko, Ege Ozguroglu, Ruoshi Liu, and Carl Vondrick. Erasedraw: Learning to insert objects by erasing them from images. In *Proceedings of the European Conference on Computer Vision*, 2024.
- Changan Chen, Puyuan Peng, Ami Baid, Zihui Xue, Wei-Ning Hsu, David Harwath, and Kristen Grauman. Action2sound: Ambient-aware generation of action sounds from egocentric videos. In *Proceedings of the European Conference on Computer Vision*, 2024a.
- Honglie Chen, Weidi Xie, Andrea Vedaldi, and Andrew Zisserman. Vggsound: A large-scale audio-visual dataset. In *Proceedings of the IEEE International Conference on Acoustics, Speech and Signal Processing*, 2020a.
- Peihao Chen, Yang Zhang, Minghui Tan, Hongdong Xiao, Deng Huang, and Chuang Gan. Generating visually aligned sound from videos. *IEEE Transactions on Image Processing*, 2020b.
- Ziyang Chen, Prem Seetharaman, Bryan Russell, Oriol Nieto, David Bourgin, Andrew Owens, and Justin Salamon. Video-guided foley sound generation with multimodal controls. *arXiv preprint arXiv:2411.17698*, 2024b.
- Ho Kei Cheng, Masato Ishii, Akio Hayakawa, Takashi Shibuya, Alexander Schwing, and Yuki Mitsufuji. Mmaudio: Taming multimodal joint training for high-quality video-to-audio synthesis. In *Proceedings of the IEEE/CVF Conference on Computer Vision and Pattern Recognition*, 2025.
- Konstantinos Drossos, Samuel Lipping, and Tuomas Virtanen. Clotho: An audio captioning dataset. In *Proceedings of the IEEE International Conference on Acoustics, Speech and Signal Processing*. IEEE, 2020.
- Yilun Du, Shuang Li, and Igor Mordatch. Compositional visual generation with energy based models. In *Proceedings of the Advances in Neural Information Processing Systems*, 2020.
- Patrick Esser, Sumith Kulal, Andreas Blattmann, Rahim Entezari, Jonas Müller, Harry Saini, Yam Levi, Dominik Lorenz, Axel Sauer, Frederic Boesel, Dustin Podell, Tim Dockhorn, Zion English, and Robin Rombach. Scaling rectified flow transformers for high-resolution image synthesis. In *Proceedings of the International Conference on Machine Learning*, 2024.
- Hugo Flores García, Oriol Nieto, Justin Salamon, Bryan Pardo, and Prem Seetharaman. Sketch2sound: Controllable audio generation via time-varying signals and sonic imitations. In *Proceedings of the IEEE International Conference on Acoustics, Speech and Signal Processing*, 2025.
- Jort F Gemmeke, Daniel PW Ellis, Dylan Freedman, Aren Jansen, Wade Lawrence, R Channing Moore, Manoj Plakal, and Marvin Ritter. Audio set: An ontology and human-labeled dataset for audio events. In *Proceedings of the IEEE International Conference on Acoustics, Speech and Signal Processing*, 2017.
- Rohit Girdhar, Alaaeldin El-Nouby, Zhuang Liu, Mannat Singh, Kalyan Vasudev Alwala, Armand Joulin, and Ishan Misra. Imagebind: One embedding space to bind them all. In *Proceedings of the IEEE/CVF Conference on Computer Vision and Pattern Recognition*, 2023.
- Bing Han, Junyu Dai, Weituo Hao, Xinyan He, Dong Guo, Jitong Chen, Yuxuan Wang, Yanmin Qian, and Xuchen Song. Instructme: An instruction guided music edit and remix framework with latent diffusion models. In *Proceedings of the International Joint Conference on Artificial Intelligence*, 2024.

- Jonathan Ho and Tim Salimans. Classifier-free diffusion guidance. In *Proceedings of the NeurIPS Workshop on Deep Generative Models and Downstream Applications*, 2021.
- Vladimir Iashin and Esa Rahtu. Taming visually guided sound generation. In *Proceedings of the British Machine Vision Conference*, 2021.
- Vladimir Iashin, Weidi Xie, Esa Rahtu, and Andrew Zisserman. Synchformer: Efficient synchronization from sparse cues. In *Proceedings of the IEEE International Conference on Acoustics, Speech and Signal Processing*, 2024.
- Yuhang Jia, Yang Chen, Jinghua Zhao, Shiwan Zhao, Wenjia Zeng, Yong Chen, and Yong Qin. Audioeditor: A training-free diffusion-based audio editing framework. In *Proceedings of the IEEE International Conference on Acoustics, Speech and Signal Processing*, 2025.
- Tornike Karchkhadze, Mohammad Rasool Izadi, and Shlomo Dubnov. Simultaneous music separation and generation using multi-track latent diffusion models. In *Proceedings of the IEEE International Conference on Acoustics, Speech and Signal Processing*, 2025.
- Tero Karras, Miika Aittala, Jaakko Lehtinen, Janne Hellsten, Timo Aila, and Samuli Laine. Analyzing and improving the training dynamics of diffusion models. In *Proceedings of the IEEE/CVF Conference on Computer Vision and Pattern Recognition*, 2024.
- Chris Dongjoo Kim, Byeongchang Kim, Hyunmin Lee, and Gunhee Kim. Audiocaps: Generating captions for audios in the wild. In *Proceedings of the Conference of the North American Chapter of the Association for Computational Linguistics: Human Language Technologies*, 2019.
- Qiuqiang Kong, Yin Cao, Turab Iqbal, Yuxuan Wang, Wenwu Wang, and Mark D Plumbley. Panns: Large-scale pretrained audio neural networks for audio pattern recognition. *IEEE/ACM Transactions on Audio, Speech, and Language Processing*, 2020.
- Saksham Singh Kushwaha and Yapeng Tian. Vintage: Joint video and text conditioning for holistic audio generation. In *Proceedings of the IEEE/CVF Conference on Computer Vision and Pattern Recognition*, 2025.
- Woosuk Kwon, Zhuohan Li, Siyuan Zhuang, Ying Sheng, Lianmin Zheng, Cody Hao Yu, Joseph E. Gonzalez, Hao Zhang, and Ion Stoica. Efficient memory management for large language model serving with pagedattention. In *Proceedings of the ACM SIGOPS Symposium on Operating Systems Principles*, 2023.
- Yaron Lipman, Ricky TQ Chen, Heli Ben-Hamu, Maximilian Nickel, and Matthew Le. Flow matching for generative modeling. In *Proceedings of The International Conference on Learning Representations*, 2023.
- Nan Liu, Shuang Li, Yilun Du, Antonio Torralba, and Joshua B Tenenbaum. Compositional visual generation with composable diffusion models. In *Proceedings of the European Conference on Computer Vision*, 2022.
- Xiulong Liu, Kun Su, and Eli Shlizerman. Tell what you hear from what you see-video to audio generation through text. In *Proceedings of the Advances in Neural Information Processing Systems*, 2024.
- Simian Luo, Chuanhao Yan, Chenxu Hu, and Hang Zhao. Diff-foley: Synchronized video-to-audio synthesis with latent diffusion models. In *Proceedings of the Advances in Neural Information Processing Systems*, 2023.
- Giorgio Mariani, Irene Tallini, Emilian Postolache, Michele Mancusi, Luca Cosmo, and Emanuele Rodolà. Multi-source diffusion models for simultaneous music generation and separation. In *Proceedings of the International Conference on Learning Representations*, 2024.
- Xinhao Mei, Chutong Meng, Haohe Liu, Qiuqiang Kong, Tom Ko, Chengqi Zhao, Mark D Plumbley, Yuexian Zou, and Wenwu Wang. Wavcaps: A chatgpt-assisted weakly-labelled audio captioning dataset for audio-language multimodal research. *IEEE/ACM Transactions on Audio, Speech, and Language Processing*, 2024.

- Andrew Owens and Alexei A Efros. Audio-visual scene analysis with self-supervised multisensory features. In *Proceedings of the European Conference on Computer Vision*, 2018.
- Julian D Parker, Janne Spijkervet, Katerina Kosta, Furkan Yesiler, Boris Kuznetsov, Ju-Chiang Wang, Matt Avent, Jitong Chen, and Duc Le. Stemgen: A music generation model that listens. In *Proceedings of the IEEE International Conference on Acoustics, Speech and Signal Processing*, 2024.
- Adam Polyak, Amit Zohar, Andrew Brown, Andros Tjandra, Animesh Sinha, Ann Lee, Apoorv Vyas, Bowen Shi, Chih-Yao Ma, Ching-Yao Chuang, David Yan, Dhruv Choudhary, DingKang Wang, Geet Sethi, Guan Pang, Haoyu Ma, Ishan Misra, Ji Hou, Jialiang Wang, Kiran Jagadeesh, Kunpeng Li, Luxin Zhang, Mannat Singh, Mary Williamson, Matt Le, Matthew Yu, Mitesh Kumar Singh, Peizhao Zhang, Peter Vajda, Quentin Duval, Rohit Girdhar, Roshan Sumbaly, Sai Saketh Rambhatla, Sam Tsai, Samaneh Azadi, Samyak Datta, Sanyuan Chen, Sean Bell, Sharadh Ramaswamy, Shelly Sheynin, Siddharth Bhattacharya, Simran Motwani, Tao Xu, Tianhe Li, Tingbo Hou, Wei-Ning Hsu, Xi Yin, Xiaoliang Dai, Yaniv Taigman, Yaqiao Luo, Yen-Cheng Liu, Yi-Chiao Wu, Yue Zhao, Yuval Kirstain, Zecheng He, Zijian He, Albert Pumarola, Ali Thabet, Artsiom Sanakoyeu, Arun Mallya, Baishan Guo, Boris Araya, Breana Kerr, Carleigh Wood, Ce Liu, Cen Peng, Dmitry Vengertsev, Edgar Schonfeld, Elliot Blanchard, Felix Juefei-Xu, Fraylie Nord, Jeff Liang, John Hoffman, Jonas Kohler, Kaolin Fire, Karthik Sivakumar, Lawrence Chen, Licheng Yu, Luya Gao, Markos Georgopoulos, Rashel Moritz, Sara K. Sampson, Shikai Li, Simone Parmeggiani, Steve Fine, Tara Fowler, Vladan Petrovic, and Yuming Du. Movie gen: A cast of media foundation models. *arXiv preprint arXiv:2410.13720*, 2024.
- Emilian Postolache, Giorgio Mariani, Luca Cosmo, Emmanouil Benetos, and Emanuele Rodolà. Generalized multi-source inference for text conditioned music diffusion models. In *Proceedings of the IEEE International Conference on Acoustics, Speech and Signal Processing*, 2024.
- Tim Salimans, Ian Goodfellow, Wojciech Zaremba, Vicki Cheung, Alec Radford, and Xi Chen. Improved techniques for training gans. In *Proceedings of the Advances in Neural Information Processing Systems*, 2016.
- Jaskirat Singh, Jianming Zhang, Qing Liu, Cameron Smith, Zhe Lin, and Liang Zheng. Smartmask: context aware high-fidelity mask generation for fine-grained object insertion and layout control. In *Proceedings of the IEEE/CVF Conference on Computer Vision and Pattern Recognition*, 2024.
- Zengjie Song and Zhaoxiang Zhang. Visually guided sound source separation with audio-visual predictive coding. *IEEE Transactions on Neural Networks and Learning Systems*, 2023.
- Stability-AI. sd3.5, 2024. URL <https://github.com/Stability-AI/sd3.5>.
- Christian J. Steinmetz and Joshua D. Reiss. pyloudnorm: A simple yet flexible loudness meter in python. In *Proceedings of the Audio Engineering Society Convention*, 2021.
- Yoad Tewel, Rinon Gal, Dvir Samuel, Yuval Atzmon, Lior Wolf, and Gal Chechik. Add-it: Training-free object insertion in images with pretrained diffusion models. In *Proceedings of the International Conference on Learning Representations*, 2025.
- Rafael Valle, Rohan Badlani, Zhifeng Kong, Sang gil Lee, Arushi Goel, Sungwon Kim, Joao Felipe Santos, Shuqi Dai, Siddharth Gururani, Aya Aljafari, Alexander H. Liu, Kevin J. Shih, Ryan Prenger, Wei Ping, Chao-Han Huck Yang, and Bryan Catanzaro. Fugatto 1: Foundational generative audio transformer opus 1. In *Proceedings of the International Conference on Learning Representations*, 2025.
- Ilpo Virtola, Vladimir Iashin, and Esa Rahtu. Temporally aligned audio for video with autoregression. In *Proceedings of the IEEE International Conference on Acoustics, Speech and Signal Processing*, 2025.
- Heng Wang, Jianbo Ma, Santiago Pascual, Richard Cartwright, and Weidong Cai. V2a-mapper: A lightweight solution for vision-to-audio generation by connecting foundation models. In *Proceedings of the AAAI Conference on Artificial Intelligence*, 2024a.

- Yongqi Wang, Wenxiang Guo, Rongjie Huang, Jiawei Huang, Zehan Wang, Fuming You, Ruiqi Li, and Zhou Zhao. Frieren: Efficient video-to-audio generation network with rectified flow matching. In *Proceedings of the Advances in Neural Information Processing Systems*, 2024b.
- Yuancheng Wang, Zeqian Ju, Xu Tan, Lei He, Zhizheng Wu, Jiang Bian, et al. Audit: Audio editing by following instructions with latent diffusion models. In *Proceedings of the Advances in Neural Information Processing Systems*, 2023.
- Max Woolf. Stable diffusion 2.0 and the importance of negative prompts for good results, 2022. URL <https://minimaxir.com/2022/11/stable-diffusion-negative-prompt/>.
- Yusong Wu, Ke Chen, Tianyu Zhang, Yuchen Hui, Taylor Berg-Kirkpatrick, and Shlomo Dubnov. Large-scale contrastive language-audio pretraining with feature fusion and keyword-to-caption augmentation. In *Proceedings of the IEEE International Conference on Acoustics, Speech and Signal Processing*, 2023.
- Yazhou Xing, Yingqing He, Zeyue Tian, Xintao Wang, and Qifeng Chen. Seeing and hearing: Open-domain visual-audio generation with diffusion latent aligners. In *Proceedings of the IEEE/CVF Conference on Computer Vision and Pattern Recognition*, 2024.
- Lvmin Zhang, Anyi Rao, and Maneesh Agrawala. Adding conditional control to text-to-image diffusion models. In *Proceedings of the IEEE/CVF International Conference on Computer Vision*, 2023.
- Yiming Zhang, Yicheng Gu, Yanhong Zeng, Zhening Xing, Yuancheng Wang, Zhizheng Wu, and Kai Chen. Foleyrafter: Bring silent videos to life with lifelike and synchronized sounds. *arXiv preprint arXiv:2407.01494*, 2024.
- Lingyu Zhu and Esa Rahtu. Visually guided sound source separation using cascaded opponent filter network. In *Proceedings of the Asian Conference on Computer Vision*, 2020.

Table of Contents

1	Introduction	1
2	Related work	2
2.1	Video-to-audio synthesis	2
2.2	Generative "add" operation	2
3	Method	3
3.1	Preliminaries	3
3.2	Problem setup: step-by-step generation in video-to-audio synthesis .	4
3.3	Formulation of target distribution with concept negation	4
4	Implementation	5
4.1	Guided flow for step-by-step generation	5
4.2	Training flow estimator for Negative Audio Guidance	6
5	Experiments	7
5.1	Evaluation setup	7
5.2	Main results	8
6	Conclusion	9
A	User study	15
B	Details of the formulation	16
C	Details of the Multi-Caps VGGSound Dataset	17
D	Training details	18
E	Sensitivity analysis of the Negative Audio Guidance coefficients	19
F	Limitation	19
G	Additional visualizations	20

A User study

In addition to the objective evaluation, we conducted a user study to perform a subjective evaluation on the Multi-Caps VGGSound dataset. We used independent generation with MMAudio-S-16k as the baseline, corresponding to the case without negative audio guidance ($\beta = 0$ in Eq. (9)), to assess the effectiveness of our proposed method. We randomly sampled five video-caption sets from the dataset (each video has five captions) and generated five audio tracks for each video using the baseline and the proposed method. As described in Section 5, we then synthesized composite audio for each video by mixing generated tracks, followed by loudness normalization. In total, we showed 60 videos to each evaluator (50 videos with individual audio tracks and 10 videos with composite audio). Human evaluators were asked to assess the quality of both individual audio tracks and the composite audio.

For the evaluation of individual audio tracks, evaluators rated each track on a scale from 1 to 5 (1-5; Poor, Subpar, Fair, Good, Excellent) across the following three aspects:

1. **Separability**: High if the audio does not contain content already present in previous audio tracks.
2. **Audio quality**: High if the audio is free from noise, distortion, or artifacts.
3. **Text fidelity**: High if the audio accurately reflects the caption.

For the evaluation of composite audio, we performed A/B testing on pairs of composite audios, one generated by the baseline and the other by our method. Specifically, five pairs of composite audios (each corresponding to the same video) were presented to evaluators, who were asked the following three questions for each pair:

1. Which audio is of higher quality?
2. Which audio has better semantic alignment with the video?
3. Which audio has better temporal alignment with the video?

For each question, evaluators could choose from three response options: "Audio A is better", "Audio B is better", and "Neutral".

We collected 320 responses for the individual audio tracks (we omitted an evaluation for the first track since the first track is identical between the two methods) and 40 responses for the composite audio from eight evaluators. Table A1 shows the results for the individual audio tracks. Our method received significantly higher ratings for separability, and marginally higher ratings for both audio quality and text fidelity. Figure A1 shows the results for the composite audio. Overall, the proposed method was preferred equally or more across all evaluation criteria.

Method	Separability \uparrow	Audio quality \uparrow	Text fidelity \uparrow
MMAudio-S-16k	2.26 \pm 1.04	2.89 \pm 1.03	2.43 \pm 1.27
MMAudio-S-16k + NAG (Ours)	3.34\pm1.11	3.30\pm1.03	3.11\pm1.28

Table A1: Average ratings for individual audio tracks generated by the baseline and our method. Each aspect is reported as mean \pm standard deviation.

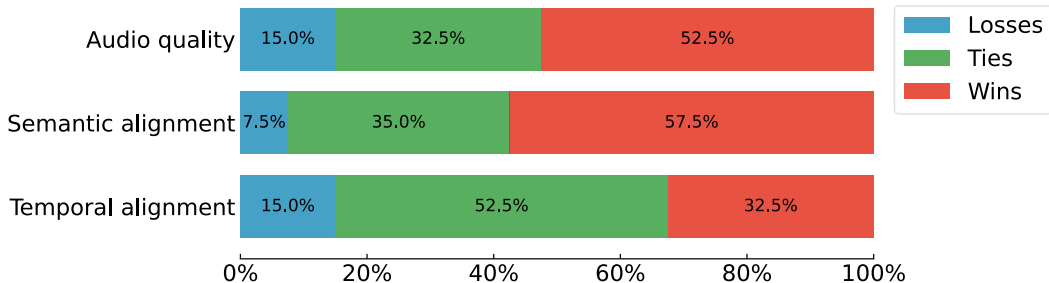


Figure A1: Results of user preference comparison between baseline and our method for composite audio. "Wins" shows the percentage of users choosing the composite audio generated by our method.

B Details of the formulation

Proof of the Equation (8)

Recall that the target distribution of each generation step can be written as:

$$\begin{aligned}
p\left(x^{(2)} \middle| V, C_2, \bar{\mathcal{E}}\left(x^{(1)}\right)\right) &\propto p\left(x^{(2)}, V, C_2, \bar{\mathcal{E}}\left(x^{(1)}\right)\right) \\
&\propto p\left(x^{(2)}, V\right) p\left(C_2 \middle| x^{(2)}, V\right) p\left(\mathcal{E}\left(x^{(1)}\right) \middle| x^{(2)}, V\right)^{-1} \\
&= p\left(x^{(2)}\right) p\left(V \middle| x^{(2)}\right) p\left(C_2 \middle| x^{(2)}, V\right) p\left(\mathcal{E}\left(x^{(1)}\right) \middle| x^{(2)}, V\right)^{-1}. \quad (\text{A1})
\end{aligned}$$

Using Bayes's theorem, we can decompose the last three terms in Eq. (A1) as follows:

$$\begin{aligned}
p\left(V \middle| x^{(2)}\right) &= \frac{p\left(x^{(2)} \middle| V\right) p(V)}{p\left(x^{(2)}\right)} \\
&\propto \frac{p\left(x^{(2)} \middle| V\right)}{p\left(x^{(2)}\right)}, \quad (\text{A2})
\end{aligned}$$

$$\begin{aligned}
p\left(C_2 \middle| x^{(2)}, V\right) &= \frac{p\left(x^{(2)} \middle| V, C_2\right) p\left(C_2 \middle| V\right)}{p\left(x^{(2)} \middle| V\right)} \\
&\propto \frac{p\left(x^{(2)} \middle| V, C_2\right)}{p\left(x^{(2)} \middle| V\right)}, \quad (\text{A3})
\end{aligned}$$

$$\begin{aligned}
p\left(\mathcal{E}\left(x^{(1)}\right) \middle| x^{(2)}, V\right) &= \frac{p\left(x^{(2)} \middle| \mathcal{E}\left(x^{(1)}\right), V\right) p\left(\mathcal{E}\left(x^{(1)}\right) \middle| V\right)}{p\left(x^{(2)} \middle| V\right)} \\
&\propto \frac{p\left(x^{(2)} \middle| V, \mathcal{E}\left(x^{(1)}\right)\right)}{p\left(x^{(2)} \middle| V\right)}. \quad (\text{A4})
\end{aligned}$$

Note that we omit terms unrelated to $x^{(2)}$, since $x^{(2)}$ is the generation target. Substituting Eqs. (A2), (A3), and (A4) into Eq. (A1), we get:

$$\begin{aligned}
p\left(x^{(2)} \middle| V, C_2, \bar{\mathcal{E}}\left(x^{(1)}\right)\right) \\
\propto p\left(x^{(2)}\right) \left(\frac{p\left(x^{(2)} \middle| V\right)}{p\left(x^{(2)}\right)}\right) \left(\frac{p\left(x^{(2)} \middle| V, C_2\right)}{p\left(x^{(2)} \middle| V\right)}\right) \left(\frac{p\left(x^{(2)} \middle| V\right)}{p\left(x^{(2)} \middle| V, \mathcal{E}\left(x^{(1)}\right)\right)}\right). \quad (\text{A5})
\end{aligned}$$

Therefore, Eq. (8) holds.

Derivation of the Negative Audio Guidance in Equation (9)

Similar to the guided flow proposed by Kushwaha and Tian [2025], we can derive the guided flow corresponding to Eq. (8) (or identically Eq. (A5)) as follows:

$$\begin{aligned}
\tilde{u}_{\theta, \psi}(x_t) &= u_{\theta}(x_t, t, \emptyset, \emptyset) + w'_1(u_{\theta}(x_t, t, V, \emptyset) - u_{\theta}(x_t, t, \emptyset, \emptyset)) \\
&\quad + w'_2(u_{\theta}(x_t, t, V, C_2) - u_{\theta}(x_t, t, V, \emptyset)) \\
&\quad + w'_3\left(u_{\theta}(x_t, t, V, \emptyset) - u_{\theta, \psi}\left(x_t, t, V, \emptyset, x^{(1)}\right)\right), \quad (\text{A6})
\end{aligned}$$

where w'_1 , w'_2 , and w'_3 are the coefficients of the guidance terms. The four terms on the right-hand side of Eq. (A6) respectively correspond to the four factors on the right-hand side of Eq. (A5).

Following the empirical results provided by Kushwaha and Tian [2025], we consider canceling out $u_\theta(x_t, t, V, \emptyset)$ for simplification. Specifically, we set $w'_1 = \alpha$, $w'_3 = \beta$, and $w'_2 = \alpha + \beta$ as follows:

$$\begin{aligned} \tilde{u}_{\theta, \psi}(x_t) = & u_\theta(x_t, t, \emptyset, \emptyset) + \alpha \left(\cancel{u_\theta(x_t, t, V, \emptyset)} - u_\theta(x_t, t, \emptyset, \emptyset) \right) \\ & + (\alpha + \beta) \left(u_\theta(x_t, t, V, C_2) - \cancel{u_\theta(x_t, t, V, \emptyset)} \right) \\ & + \beta \left(\cancel{u_\theta(x_t, t, V, \emptyset)} - u_{\theta, \psi}(x_t, t, V, \emptyset, x^{(1)}) \right), \end{aligned} \quad (\text{A7})$$

which yields Eq. (9).

C Details of the Multi-Caps VGGSound Dataset

As described in Section 5.1, we generated five captions for each video in the test split of the VGGSound dataset using Qwen2.5-VL [Bai et al., 2025], resulting in 76,105 video-caption pairs (15,221 videos \times 5 captions). Figure A2 shows an overview of the dataset construction workflow. We adopted a two-step approach to ensure that the captions follow a unified format across all videos (i.e., short, simple sentences, each describing a distinct audio event). Specifically, given an input video, we first generated multiple possible audio captions in a free-form text, describing the audio events likely present in the video. Next, we reformatted the output into a structured JSON format using the generation of structured outputs (we referred to the implementation of vLLM [Kwon et al., 2023]). The full prompt we used in the first step is shown in Fig. A3. While Qwen2.5-VL generates multiple captions in response to this prompt, the output may vary between inferences. To standardize this, the second step converts the results into a unified JSON format that lists only the captions. This structured format is well-suited for use as text conditions in text-conditional video-to-audio models. Figure A4 provides examples of video and multiple caption pairs.

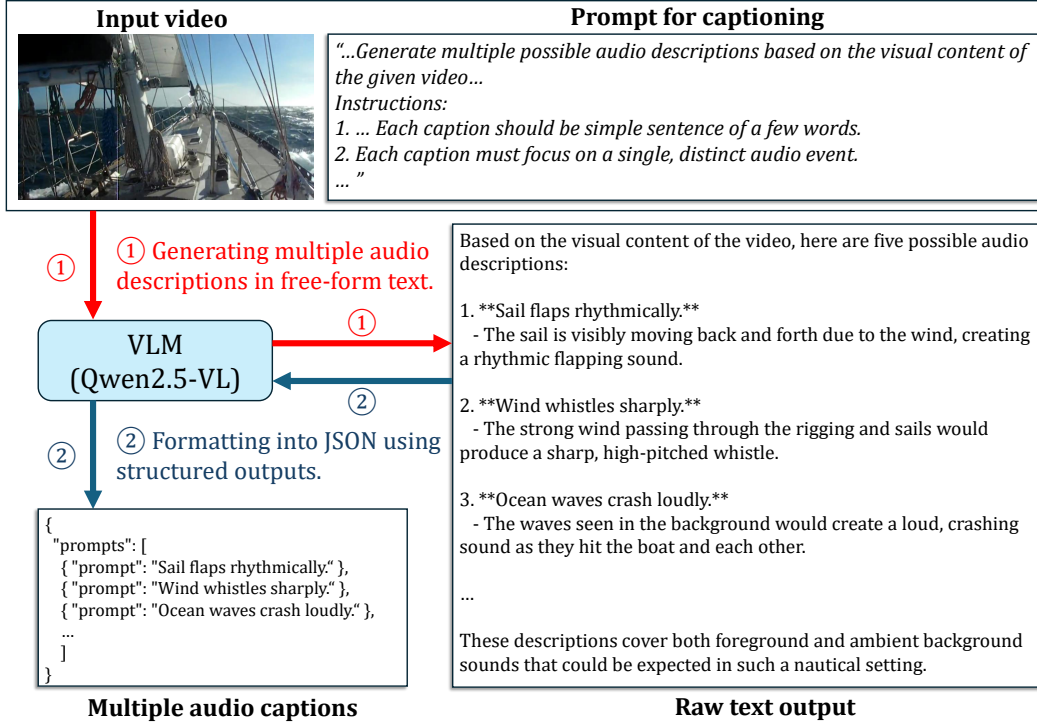


Figure A2: Overview of the dataset construction pipeline. Multiple audio captions were generated for each video using Qwen2.5-VL via a two-step process: free-form captioning followed by structured JSON formatting. The input prompt on the top is simplified; see Fig. A3 for the full version.

“Task:

You are a professional sound effects creator. Generate multiple possible audio descriptions based on the visual content of the given video. Each description should focus on a single, distinct audio event, and each could be either a foreground sound or an ambient background sound. Foreground sounds are the sounds that are directly depicted in the video (e.g., a dog barking, footsteps). Ambient background sounds are the sounds that could be inferred or imagined from the video’s context but not explicitly shown (e.g., distant wind, soft city hum).

Examples:

- #1 The dog barks loudly.
#2 The river flows gently.

Instructions:

1. Use the format: ‘Noun + Verb + Adverbs’ (adverbs are optional). Each caption should be simple sentence of a few words.
2. Each caption must focus on a single, distinct audio event.
3. Begin each caption with ‘#N’, where N is the index of the description.
4. AVOID DUPLICATES, and provide up to 5 descriptions per video.”

Figure A3: Full prompt for generating multiple possible audio captions.




Video	Generated captions
	<p>0: “Ocean waves crash loudly.” 1: “Sail flaps rhythmically.” 2: “Wind whistles sharply.” 3: “Ropes creak softly.” 4: “Metal clanks intermittently.”</p>
	<p>0: “Pheasant cackles softly.” 1: “Grass rustles gently underfoot.” 2: “Wings flutter faintly.” 3: “Birds chirp in the distance.” 4: “Wind whispers through the grass.”</p>
	<p>0: “Engine roars powerfully.” 1: “Wheels grind heavily on pavement.” 2: “Horn blasts loudly.” 3: “People chatter excitedly.” 4: “Bicycles click softly as they move.”</p>

Figure A4: Examples of the Multi-Caps VGGSound dataset. We added multiple captions to the test split of the VGGSound dataset using Qwen2.5-VL shown in Figure A2.

D Training details

We followed the training setup of MMAudio [Cheng et al., 2025] for training the ControlNet. We used the AdamW optimizer with a learning rate of 10^{-4} , $\beta_1 = 0.9$, $\beta_2 = 0.95$, and a weight decay of 10^{-6} , and trained the network for 200K iterations with a batch size of 512. Compared to MMAudio’s default of 300K iterations, we reduced the number of training steps to 200K, as we observed earlier convergence in our experiments. We only updated the parameters of the ControlNet while fixing the pre-trained parameters of MMAudio, enabling more efficient training. For learning rate scheduling, we applied a linear warm-up over the first 1K steps up to 10^{-4} , followed by two reductions, each by

a factor of 10, after 80% and 90% of the total training steps. We used mixed precision training with bf16 for the training efficiency and trained on 8 H100 GPUs. The entire training process, including evaluation on the validation and test sets every 20K iterations, took approximately 10 hours. After training, we applied post-hoc EMA [Karras et al., 2024] with a relative width $\sigma_{\text{rel}} = 0.05$ to obtain the final parameters of the ControlNet.

E Sensitivity analysis of the Negative Audio Guidance coefficients

We conducted a sensitivity study on the guidance coefficients of NAG (α, β in Eq. (9)). Specifically, we varied $\alpha \in \{3.5, 4.5\}$ and $\beta \in \{0.0, 1.0, 1.5, 2.0\}$ and generated audio tracks for all combinations of these parameter pairs. The individual audio tracks and their corresponding composite audio were evaluated using the same setup and metrics described in Section 5.1. We used CLAP A-A for audio independency, IS and FD_{PANNs} for audio quality, CLAP T-A for text fidelity, IB-score for semantic alignment with video, and DeSync for temporal alignment with video.

The results are summarized in Table A2. Both CLAP A-A and CLAP T-A for the individual audio tracks consistently improved with increasing β . This indicates that NAG effectively generates well-separated audio tracks with enhanced text alignment, likely due to reduced contamination from other audio concepts. The best FD_{PANNs} and IB-score are achieved at $\beta = 1.0$, indicating that a moderate strength of NAG also enhances audio fidelity and semantic alignment with video. Using small α slightly deteriorates performance across all metrics, potentially due to the degradation of the performance of the base MMAudio (the default CFG strength recommended by Cheng et al. [2025] is 4.5). Considering trade-offs among these metrics, we selected $\alpha = 4.5$ and $\beta = 1.5$ as our default setting.

Method	Individual Audio Tracks			Composite Audio			
	CLAP A-A↓	IS↑	CLAP T-A↑	$\text{FD}_{\text{PANNs}}\downarrow$	IS↑	IB-score↑	DeSync↓
$\alpha = 3.5, \beta = 0.0$	79.46	12.27	28.34	7.83	10.37	27.80	0.45
$\alpha = 3.5, \beta = 1.0$	75.22	12.06	28.75	7.52	10.17	27.94	0.45
$\alpha = 3.5, \beta = 1.5$	73.45	11.84	28.89	7.62	9.90	27.62	0.45
$\alpha = 3.5, \beta = 2.0$	71.97	11.62	29.01	7.84	9.69	27.28	0.45
$\alpha = 4.5, \beta = 0.0^*$	79.75	12.47	28.36	7.76	10.42	28.13	0.43
$\alpha = 4.5, \beta = 1.0$	76.21	12.22	28.69	7.30	10.38	28.38	0.43
$\alpha = 4.5, \beta = 1.5^\dagger$	74.74	12.00	28.79	7.32	10.21	28.15	0.43
$\alpha = 4.5, \beta = 2.0$	73.44	11.80	28.88	7.52	9.92	27.88	0.43

Table A2: Sensitivity study on the guidance coefficients of NAG (α, β in Eq. (9)). The first three metrics are computed on the individual audio tracks, and the last four are computed on the composite audio. *: identical to the independent generation of MMAudio-S-16k with the default CFG strength of 4.5. †: our default setting.

F Limitation

In terms of individual audio track quality, our method marginally improves text fidelity but slightly degrades audio quality. While NAG effectively eliminates contamination from other audio tracks, the outputs sometimes exhibit poor alignment with the text captions or suffer from low quality, such as silence or muffled sound. This may stem from limitations in the base MMAudio model, particularly with handling subtle or rare sounds (e.g., “Carpet rustles gently”, “Wings flap gently”, “Snowflakes fall silently”, “Crowd murmurs quietly”). Even when conditioned only on such text prompts, MMAudio often produces hums, noise, or unnaturally loud sounds, likely due to the scarcity of such audio events in its training data. These mismatches suggest a domain gap between Multi-Caps VGGSound and MMAudio’s training distribution. Since NAG only guides generation away from previous outputs, overall quality and text alignment rely heavily on the base TV2A model’s capabilities. The effectiveness of our proposed method would likely be more pronounced if the base model supported a broader range of text prompts (i.e., ideally broad enough to match the range supported by LLMs) and could generate more diverse audio outputs, even for the same video input.

G Additional visualizations

Figure A5 shows additional spectrogram visualizations comparing MMAudio, MMAudio + negative prompting, and MMAudio + NAG.

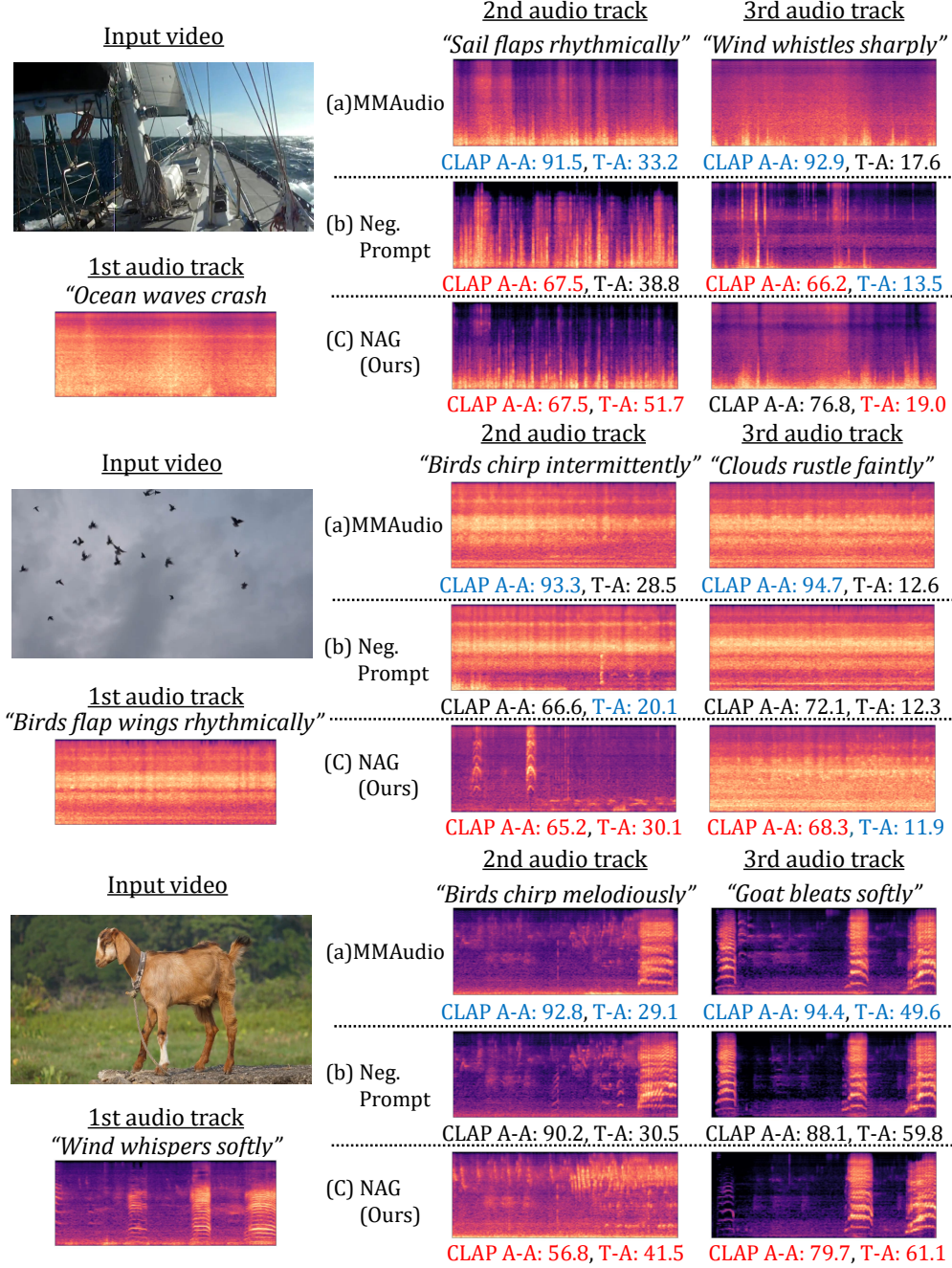


Figure A5: Additional spectrogram visualization. Our proposed method effectively suppresses previously generated sounds in subsequent steps while maintaining high alignment with the text prompts. The best and worst CLAP A-A and T-A scores are highlighted in red and blue, respectively.